Planetary and Space Science 257 (2025) 106051

Contents lists available at ScienceDirect

Planetary and Space Science

journal homepage: www.elsevier.com/locate/pss

An Arctic analogue for the future exploration of possible biosignatures on Enceladus

F. Franchi [a,b,*], M. Túri [c], G. Lakatos [c,d,e], K.K. Rahul [c], D.V. Mifsud [c], G. Panieri [f], R. Rácz [c], S.T.S. Kovács [c], E. Furu [c], R. Huszánk [c], R.W. McCullough [g], Z. Juhász [c,**]

[a] Dipartimento di Scienze della Terra e Geoambientali, Università degli Studi di Bari Aldo Moro, Bari, Italy
[b] School of Geosciences, University of the Witwatersrand, Johannesburg, South Africa
[c] HUN-REN Institute for Nuclear Research (Atomki), Debrecen, Hungary
[d] Institute of Chemistry, University of Debrecen, Hungary
[e] Doctoral School of Chemistry, University of Debrecen, Hungary
[f] Department of Geosciences, UiT – The Arctic University of Norway, Tromsø, Norway
[g] Department of Physics and Astronomy, School of Mathematics and Physics, Queen's University Belfast, Belfast, United Kingdom

ARTICLE INFO

Keywords:
Methane
Hydrogen
Biosignatures
Enceladus
Astrobiology
Mass spectrometry

ABSTRACT

Methane-rich emissions to the seafloor along the Arctic mid-oceanic ridge hold strong astrobiological significance, as they may represent analogues of putative hydrothermal vent environments on Enceladus. Although such environments on Enceladus would be ideal to sample in future astrobiological missions, this may not be possible due to technological and logistical limitations. As such, searching for biosignatures in the more readily sampled cryovolcanic plumes or Enceladus' icy shell is preferable. In this regard, the Arctic Ocean, where the geologically active seafloor is covered by thousands of metres of salty water and sealed by an ice cap, is a unique terrestrial analogue of Enceladus. In the present study, we have sought to determine whether any geochemical biosignatures associated with methane cycling (e.g., elevated methane concentrations, carbon isotopic fractionation) can be detected in Arctic ice and seawater samples using mass spectrometric techniques similar to those likely to be included in the payloads of planned missions to Enceladus. Our results have shown that, although no unequivocal evidence of methane could be detected in our Arctic samples, the carbon isotopic composition of carbon dioxide gas and the oxygen isotopic composition of water vapour emitted from the Arctic samples could indeed be measured. Furthermore, an excess of molecular hydrogen with abundances comparable to the composition of Enceladus' southern pole plume was possibly observed in one of the Arctic ice samples. These results have implications for detectable indirect geochemical evidence of putative ecosystems of hydrogenotrophic methanogenic life on the seafloor of Enceladus and justify future efforts at method development and refinement using apparatus similar to that likely to be included in the payloads of future missions.

1. Introduction

Over the past five decades, the idea that Earth is unique in the Solar System as the only body on which liquid water exists has been overturned by the discovery of several so-called 'ocean worlds' which host vast quantities of liquid water in their sub-surfaces. One such ocean world is the Saturnian moon Enceladus, where compelling evidence for the presence of liquid water was found by the *Cassini-Huygens* probe and subsequent investigations (Postberg et al. 2009, 2011; Iess et al. 2014). Specifically, sampling of the cryovolcanic plume ejected from Enceladus' southern pole by the Ion and Neutral Mass Spectrometer (INMS; Waite et al., 2004) and the Cosmic Dust Analyser (CDA; Srama et al., 2004) aboard *Cassini-Huygens* revealed the presence of water ice, methane and other carbon-bearing molecules, molecular hydrogen, and molecular nitrogen (Porco et al. 2006; Waite et al. 2006; McKay et al. 2012; Postberg et al. 2018; Khawaja et al. 2019). Sodium and potassium salts (Postberg et al. 2009) and, more recently, phosphate salts (Postberg et al. 2023) have also been detected in the ice grains by the CDA, suggesting that Enceladus' plumes are frozen seawater originating from a sub-surface ocean.

* Corresponding author. Dipartimento di Scienze della Terra e Geoambientali, Università degli Studi di Bari, Aldo Moro, Bari, Italy.
** Corresponding author. HUN-REN Institute for Nuclear Research (Atomki), Debrecen, Hungary.
E-mail addresses: fulvio.franchi@uniba.it (F. Franchi), zjuhasz@atomki.hu (Z. Juhász).

https://doi.org/10.1016/j.pss.2025.106051
Received 4 September 2024; Received in revised form 17 January 2025; Accepted 21 January 2025
Available online 23 January 2025

Moreover, Enceladus is the only Saturnian moon with proven endogenic activity (Hsu et al. 2015; Waite et al. 2017; Mitri et al. 2021), and is characterised by an ice cover whose thickness varies from 35 to 40 km down to just a few kilometres at the south pole (Hemingway et al. 2018), an internal ocean (Postberg et al. 2009, 2011) with hydrothermal vents acting as sources of energy and nutrients at its depths (Bouquet et al. 2015; Hsu et al. 2015), and possibly the formation of clathrates (Bouquet et al. 2015). As such, Enceladus in principle contains all the key ingredients to sustain chemoautotrophic pathways for the emergence of life (Mitri et al. 2018, 2021; Carrizo et al. 2022) and is a favoured target for future astrobiological exploration (Taubner et al. 2018; Cable et al. 2021; Carrizo et al. 2022). Indeed, several fly-by missions of Enceladus have been proposed with the aim of using mass spectrometers to indirectly identify biosignatures within the sub-surface ocean by sampling the gases and ice grains within the plume (e.g., Reh et al. 2016; Klenner et al. 2024).

In this present communication, we focus on the technical feasibility of detecting and characterising evidence of methane cycling on Enceladus as an indicator for the present and past habitability of this ocean world (McKay et al. 2012; Carrizo et al. 2022). On Earth, methane generation is the result of both biological and abiotic processes, but often (if not always) carries implications for microbial communities. For instance, biogenic methane formation is mediated by consortia of methanogenic archaea or by the thermogenic breakdown of buried organic matter. On the other hand, the abiotic formation of methane results from Fischer-Tropsch-type reactions fuelled by molecular hydrogen generated through serpentinization processes (Oze and Sharma, 2005; Oehler and Etiope, 2017). Serpentinization-derived hydrogen can sustain hydrogenotrophic methanogenic ecosystems in hydrothermal vents at the seafloor (e.g., Mayhew et al., 2013). Furthermore, gas vented at the seafloor may sustain communities of chemoautotrophs and the bio-induced or bio-controlled precipitation of authigenic materials such as calcite and aragonite (Riding and Virgone, 2020).

If conditions on Enceladus were ever favourable for life to exist, then it is possible to argue that fossil (or extant) evidence for it could be found in geological materials associated with vents, seeps, and gas hydrates (Carrizo et al. 2022). Since these vents and seeps are at the bottom of a ca. 20–30 km-deep ocean (Hemingway et al. 2018; Park et al. 2024) covered by up to ca. 35–40 km of ice, it is plausible that molecular signatures of life can be trapped in the icy outer shell as a result of convective motion that would transfer molecules emitted by seafloor venting to the ice-ocean interface before becoming entrained within plumes due to ice convective motion (Bouquet et al. 2015). The characterisation of the isotopic composition of methane seeping at the seafloor will also prove crucial in discriminating abiotic sources of hydrocarbons on Enceladus from potentially biological ones. Although such a characterisation could, in principle, be achieved by measuring stable isotopes associated with the depletion of ^{13}C by biological activity, it is to be noted that stable isotope compositional analysis alone cannot unambiguously indicate the source of methane (McCollom and Seewald, 2006; Milkov and Etiope, 2018), particularly if the isotopic composition of the CO_2 undergoing reduction is not known. Instead, it may be preferable to combine standard isotopic analysis with the quantification of the ratio of methane to other more complex hydrocarbons (Milkov and Etiope, 2018), or with clumped isotopic analysis of $^{13}CH_3D$ molecules (Wang et al. 2015; Douglas et al. 2017).

Enceladus is a high priority target for both ESA and NASA, as demonstrated by the proposed ESA L4 mission and the NASA Planetary Science and Astrobiology Decadal Survey 2023–2032. This unparalleled interest has urgently spurred the development of methodologies by which the unambiguous detection of potential biosignatures can be confirmed. Recent work has shown that direct evidence for microbial life could be found by proposed fly-by missions, such as the *Enceladus Life Finder* (Reh et al. 2016), at altitudes >1 km by analysing ice grains within plume material using mass spectrometry (Dannenmann et al. 2023; Klenner et al. 2024). Nonetheless, novel methodologies should be developed that also focus on searching for indirect geochemical evidence within Enceladus' icy shell that is indicative of hydrothermal activity and methane cycling within the sub-surface ocean. These novel methodologies should be tested to assess whether the sought-after geochemical evidence is likely to be detectable by methods comparable to those in the payloads of future missions (Mitri et al. 2018, 2021; MacKenzie et al. 2021).

One way of assessing the practicability of detecting geochemical evidence of life on Enceladus is to study a terrestrial analogue of this icy moon where a geologically active seafloor is covered by thousands of metres of salty water and sealed by an ice sheet. One such analogue is the Arctic Ocean, where vents and seeps are found along active margins in an ocean covered by ice for most of the year (Panieri et al. 2017, 2022). In this present communication, we have analysed the natural ice and seawater from the Arctic Ocean off the coastline of Svalbard (Fig. 1) with mass spectrometric and isotope geochemical techniques with the aim of identifying direct and indirect evidence of methane seepage (possibly from gas hydrate dissociation) and, also, to qualitatively assess the biogenicity of the gas. This work therefore aims to address, with an astrobiological perspective, the following questions: (i) is it possible to detect evidence of methane venting and seepage in the ice capping the ocean, and (ii) is it possible to demonstrate clear isotopic fractionations using spectrometric methods comparable with those likely to be included in the payloads of future missions?

2. Study area, materials, and methods

2.1. Study area

The West Svalbard continental slope represents one of the northernmost gas hydrate provinces in the world, and is situated on hot (>115 mW m^{-2}) and relatively young oceanic crust (Engen et al. 2008). The site investigated during the oceanic expedition lies at the southernmost extent of the Vestnesa Ridge, on the Svalbard continental slope (Fig. 1). The Vestnesa Ridge is a 100 km-long submarine sediment drift that extends from the continental slope and elongates in a SE-NW (eastern segment) to E-W (western segment) bending direction, where

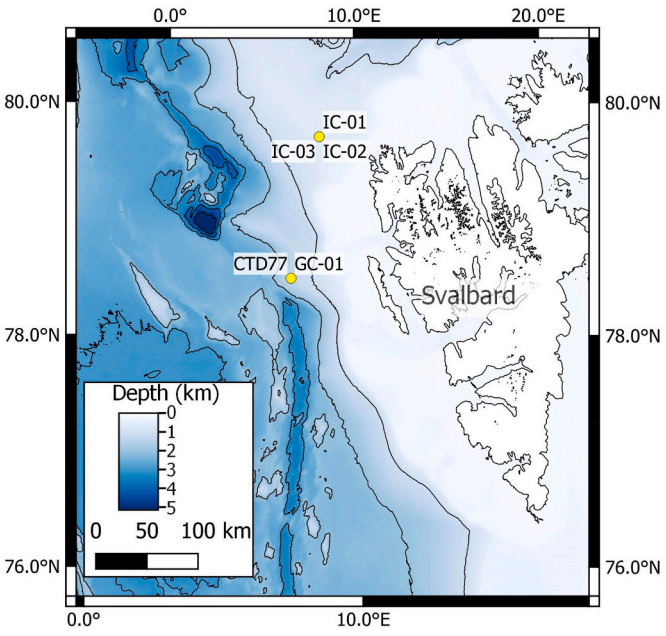

Fig. 1. Map of the study area, with sampling sites highlighted (IC = ice samples; CTD = water samples collected using a conductivity, temperature, and depth probe; GC = gas hydrate sample collected using a gravity corer).

the crest of the ridge lies at 1200–1300 m water depth (Bünz et al. 2012; Plaza-Faverola et al. 2015). Gas hydrates are very common in the area as revealed by several seismic studies (Eiken and Hinz, 1993; Posewang and Mienert, 1999; Vanneste et al. 2005) and direct sampling (Panieri et al. 2017), with fluid leakage structures including those along faults having first been detected in 2001 (Vanneste et al. 2005). Faults control the ascent of fluids and the distribution of seeps on the Vestnesa Ridge (Vanneste et al. 2005; Plaza-Faverola et al. 2015) and chronology obtained from uranium-thorium dating of seep carbonates suggests glacial tectonics induced by ice sheet fluctuations on Svalbard mainly controlled the release of methane from the Vestnesa Ridge (Himmler et al. 2019). Being situated within a few kilometres of the mid-oceanic ridge, the Vestnesa Ridge gas hydrate and vents system likely interacts with warm fluids whose circulation is driven by hydrothermal activity, making this gas hydrate system unique on Earth (Bünz et al. 2012).

2.2. Sampling

Samples were collected during the AKMA2-OceanSenses Research Expedition (11–23 May 2022) to the Barents Sea and Arctic Ocean, aboard the research vessel Kronprins Haakon (Panieri et al. 2022). Ice and surface water were sampled from the ice pack at coordinates 79° 56.92′ N - 8° 05.96′ E (Fig. 1). Four cores were drilled into the pack at the corners of a 20 × 20 m square using a corer and a hand-drill and collected for analysis. The maximum ice thickness was found to be 1.38 m. Water was also collected from the drill holes for compositional analysis and comparison with the ice cores. On board, the ice cores were sliced and stored in vacuum bags at −20 °C. Ice samples 2.2 and 3.1B were collected near the ice-water interface at depths of 1.12–1.25 m and 1.21–1.27 m, respectively (Table 1). Ice sample 3.9B represents the top of the ice pack, at an average depth of 5 cm from the snow-ice interface. Samples of deep water (CTD 01 and CTD 04) were collected along the Vestnesa Ridge (78° 41′ N - 7° 00’ E) at a depth of 1392 m using a conductivity, temperature, and depth (CTD) probe. Shallow (<1 m from the sediment-water interface) gas hydrates were sampled in the same area using a gravity corer; the gas hydrates from the core catcher were placed in a sampling bottle, and the bottle was submerged upside-down into a bucket with seawater. The strong degassing drove the water outside the bottle that was then closed trapping only gas inside. The gas bottle was then transferred to the laboratory and gas was sampled with a syringe and transferred into vials for transport (GS 1B).

Table 1
Summary of the samples collected and analysed.

Sample	Description	Coordinates		Station ID
		Longitude	Latitude	
CORE1	Seawater sample from the hole of core 1 ***Depth:*** *surface water* Fig. 1 Label: IC-01	08° 11.045′	79° 56.929′	CAGE22-2-KH-03-IC-01
ICE 2.2	Ice sample from the bottom of core 2 ***Depth:*** *1.15-1.25 m below surface level* Fig. 1 Label: IC-02	08° 11.045′	79° 56.929	CAGE22-2-KH-03-IC-02
ICE 3.1B	Ice sample from the bottom of core 3 ***Depth:*** *1.21-1.27 m below surface level* Fig. 1 Label: IC-03	08° 11.045′	79° 56.929′	CAGE22-2-KH-03-IC-03
ICE 3.9B	Ice sample from the surface of core 3 ***Depth:*** 5 cm *from the snow-ice interface* Fig. 1 Label: IC-03	08° 11.045′	79° 56.929′	CAGE22-2-KH-03-IC-03
GS 1B	Gas collected from dissociation of clathrate ***Depth:*** *1249 m below sea level* Fig. 1 Label: GC-01	07° 00.826′	78° 42.061′	CAGE22-2-KH-03-GC-01
CTD 01	Seawater sample collected 10 m above seafloor ***Depth:*** *1392 m below sea level* Fig. 1 Label: CTD77	07° 00.855′	78° 42.085′	CAGE22-2-KH-03-CTD-77
CTD 04	Seawater sample collected 10 m above seafloor ***Depth:*** *1392 m below sea level* Fig. 1 Label: CTD77	07° 00.855′	78° 42.085′	CAGE22-2-KH-03-CTD-77

2.3. Geochemical analysis

The hydrogen and oxygen stable isotopic compositions of the melted ice samples were determined at the HUN-REN Institute for Nuclear Research in Debrecen, Hungary using off-axis integrated-cavity output spectroscopy (OA-ICOS; LGR LWIA-24i, ABB-Los Gatos Research) in line with the IAEA Laboratory Information Management System Protocol (Coplen, 2004). Samples and laboratory standards were pipetted into 1.5 mL vials from which a 1 μL volume of water was injected into the vaporiser of the laser analyser, where it underwent evaporation at 80 °C under a low vacuum of about 1 mbar. A high-finesse optical cavity with two high-reflectivity (99.99%) mirrors acts as the spectroscopic absorption cell, which has an effective path length of 2500 m allowing for significant enhancement of light absorption as it traverses the optical cavity. Measured absorption spectra could then be used to determine the stable isotopic composition of the melted ice sample.

Although nine injections from each vial were used to generate spectra, only the latter five measurements were used to determine the final isotopic composition of the samples so as to minimise any memory effects. Additionally, all samples were measured in triplicate. The isotopic compositions of the laboratory standards used during this analysis are provided in the supplementary information document. Measured isotopic compositions were expressed in the usual δ^2H and $\delta^{18}O$ notation relative to Vienna Standard Mean Ocean Water (V-SMOW; Coplen, 1994), and the uncertainty (1-σ) based on control samples over a two-year period is better than 0.6‰ and 0.08‰ for δ^2H and $\delta^{18}O$, respectively. In addition to the hydrogen and oxygen stable isotopic composition analysis, pH measurements of the melted ice and seawater samples were also performed using an Orion Star A216 pH meter with a glass electrode.

2.4. Mass spectrometric analysis

The relative composition of gases emitted during the melting of the Arctic ice samples was ascertained via 70 eV electron impact quadrupole mass spectrometry (QMS; HIDEN, HAL IV, Model 201) across a mass range of 1–50 amu in experiments that were also performed at the HUN-REN Institute for Nuclear Research. Ice samples were placed in a transparent plastic container which was then rapidly evacuated to pressure levels of ca. 10^{-2} mbar by means of an attached scroll pump and subsequently sealed (Fig. 2). Over time, the ice proceeded to melt and previously trapped gases and vapours accumulated in the upper portion of the plastic container. Once the ice samples had fully melted, gases were directed via a needle valve into an ultrahigh-vacuum chamber fitted with the QMS (Rácz et al. 2024), causing a near two order-of-magnitude increase in the pressure of the chamber from background levels of (6–9) × 10^{-9} mbar to (1–2) × 10^{-7} mbar. In the case of the Arctic seawater and gas samples, the entire sampling bottle was placed into the plastic container which was then evacuated and sealed. The lid of the sampling bottle was then broken by means of a vacuum-tight ‘punch’ (Fig. 2), thus mimicking the scenario in which sub-surface ocean water ‘punches’ through the icy shell of Enceladus and escapes as a plume during cryovolcanism. Gases and vapours were subsequently introduced into the ultrahigh-vacuum chamber for QMS

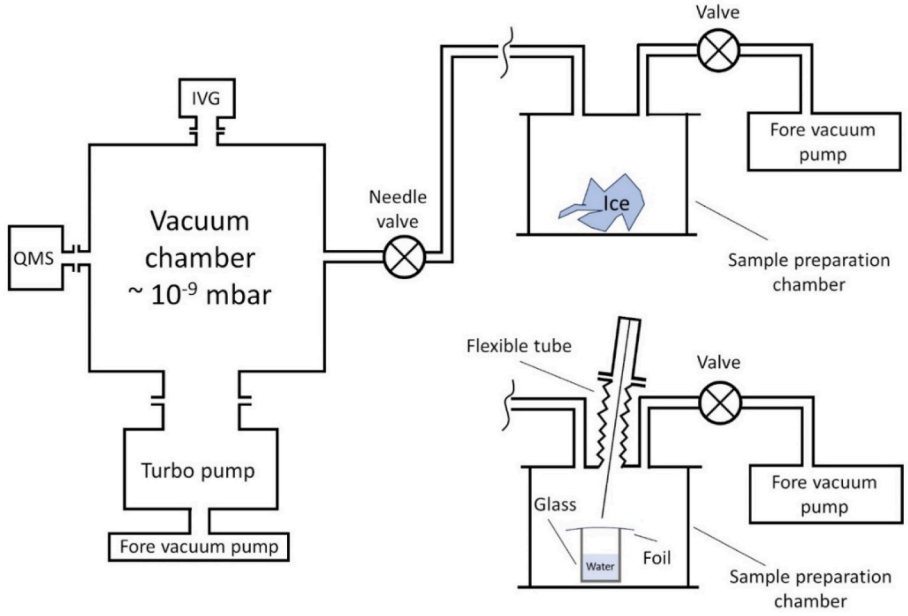

Fig. 2. Schematic representation of the method and apparatus used to measure the mass spectra of gases emitted by melted ice samples (top-right) and seawater and gas samples (bottom-right) using an ultrahigh-vacuum chamber fitted with a QMS (left). Vacuum levels in that chamber were measured using an ionisation vacuum gauge (IVG).

analysis in the same way as for the ice samples.

QMS analysis was performed by measuring integer masses sequentially using an ion counting secondary electron multiplier (SEM), which counts the number of ions striking it per second, with the full mass range being scanned in <2 s. Of course, scanning could be performed at higher mass resolutions; however, this would drastically increase the scan time of the full mass range which is not ideal from the perspective of future missions to Enceladus, which may only have very limited times to sample the near-surface environment during fly-bys. Fast scan times (on the order of seconds) are desirable so as to obtain spatial information on the materials ejected by plumes during fly-bys which, for spacecraft entering at high speed, would typically last several minutes in the upper atmospheres of outer Solar System moons (Reh et al., 2016; Mousis et al., 2022). Naturally, this sets some limitations on the resolution of the scan and the selected mass range and so investigations should instead focus on the mass range most likely to provide useful information on the presence or absence of potential biosignatures. QMS measurements were also repeated using a Faraday cup detection method, which requires a significantly longer scan time compared to SEM detection. The results obtained were essentially identical to those obtained using SEM detection but with somewhat lower statistics, and so they have been excluded from the present analysis. The description of the treatment of the QMS data is lengthy and elaborate, and thus the interested reader is directed to the supplementary information document for more details.

3. Results

3.1. Geochemical analysis

Measured pH values for the ice and water samples are given in Table 2. Note that all samples, with the exception of CTD 04, had pH values lower than that of standard seawater (8.1–8.3; Marion et al. 2011), indicating their relative acidity, and samples roughly increased in acidity with decreasing depth. A number of geochemical processes could contribute to this increased acidity at shallower depths, such as ocean acidification as a result of increased carbon dioxide emissions from anthropogenic activity (Orr et al. 2005), or salt expulsion and mineral precipitation as the brine within the ice becomes more concentrated (Veselý et al., 2024). Indeed, the measured conductivity of the melted ice sample ICE 2.2 is lower than that of standard seawater, thus indicating that it underwent salt expulsion during its formation (Table 3). However, it is to be noted that the results are at least consistent with the idea of methane being released at the seafloor and being oxidised via biological or abiotic processes to carbon dioxide during its ascent (James et al. 2016 and references therein).

The measured isotopic compositions of the ice and seawater samples revealed that the surface water sample CORE1 exhibited δ^2H and $\delta^{18}O$ values comparable to the standard, within 1-σ (Table 3). The ice sample ICE 2.2 exhibited significant enrichments of ^2H and moderate-to-large enrichments of ^{18}O, with δ^2H and $\delta^{18}O$ values of 17.43‰ and 1.959‰, respectively; while the deep ocean water CTD 01 exhibited noticeably negative δ^2H and $\delta^{18}O$ values. These results are likely indicative of the

Table 2
Measured pH values for the acquired Arctic ice and water samples.

Sample	Depth (m)	Measured pH
CORE1	Surface water	7.93
ICE 2.2	1.15	7.25
ICE 3.1B	1.21	8.03
ICE 3.9B	0.05	6.70
CTD 04	1392	8.25
Ultra-Pure Water (control)	–	5.35

Table 3
Isotopic composition of Arctic water and ice samples. Note that δ^2H and $\delta^{18}O$ values are expressed in ‰ relative to V-SMOW.

Sample	Depth (m)	$\delta^2H \pm 1\text{-}\sigma$ (‰)	$\delta^{18}O \pm 1\text{-}\sigma$ (‰)	Conductivity (mS cm^{-1})
CORE1	Surface	1.76 ± 0.12	0.083 ± 0.081	37.3
ICE 2.2	1.15	17.43 ± 0.13	1.959 ± 0.055	4.0
CTD 01	1392	−9.05 ± 0.02	−1.324 ± 0.041	45.6
Standard	-	0.91 ± 0.75	−0.065 ± 0.098	12.5

isotopic fractionation effect that occurs during the freezing of water in which heavy isotopes are preferentially incorporated into the ice phase (Souchez and Tison, 1987; Lehmann and Siegenthaler, 1991; Toyota et al. 2013). However, if this abiotic source of fractionation were the only control on the isotopic composition of the seawater samples, then we would expect an isotopic gradient to be established at the ice-seawater interface which would result in the surface water samples being enriched in lighter isotopes compared to deep ocean water samples, which is not the case here (Table 3). As such, other factors (possibly including metabolic processes) must be contributing to the observed δ^2H and $\delta^{18}O$ values.

3.2. Mass spectrometric analysis

The abundances of several gas species of interest (CH_4, C_2H_6, H_2, N_2, O_2, CO_2, Ar, and Ne) trapped or dissolved within the Arctic water and ice samples was assessed by QMS (Fig. 3, Table 4). We note that the H_2O content measured in the mass spectra does not yield any useful information, as this is controlled simply by the volume ratio of the melted ice sample and its container. The composition of the gases emitted from the ice sample ICE 2.2, which was collected from the ice-seawater interface, is the most similar to that of air, with the notable exception of a relatively high molecular hydrogen abundance, for which the associated uncertainty of measurement is small. Further confirmatory evidence of the identification of molecular hydrogen in this sample came in the form of control experiments in which the emitted gas composition of a sample of frozen and rethawed ultra-pure water exhibited only trace quantities of molecular hydrogen.

Although molecular hydrogen may have been sourced from the melted ice itself (Herr et al. 1981; Herr, 1984), it is also possible that it was generated within the experimental apparatus as a result of the dissociation of water molecules in contact with metallic surfaces (Raza et al. 2022). Indeed, the reduced abundance of carbon dioxide in this sample compared to others is in line with this latter scenario since the hydrides formed as a result of reactions between the metallic surfaces and water may absorb a large amount of carbon dioxide. Furthermore,

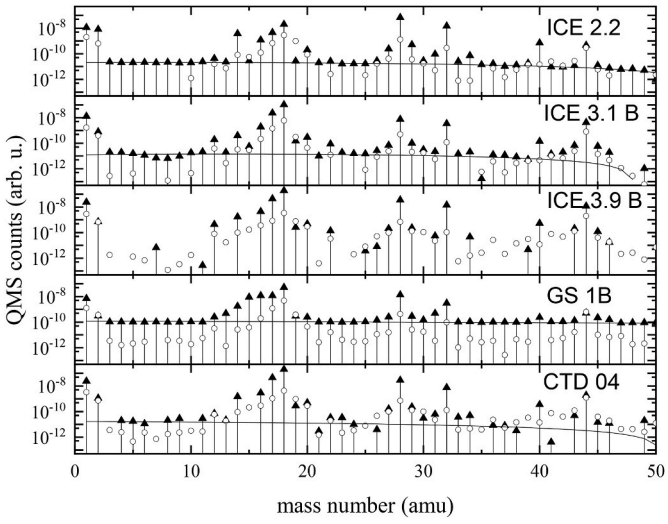

Fig. 3. Mass spectra of ice samples ICE 2.2 (1.15 m depth), ICE 3.1B (1.21 m depth), ICE 3.9B (0.05 m depth), of gas from clathrates GS 1B (collected at the seafloor at a depth of 1249 m below sea level), and of deep water CTD 04 (collected at the seafloor at a depth of 1392 m below sea level). The values shown here (black triangles) are averaged over several tens to hundreds of scans. The spectra depicted here are the result of subtracting the mass spectra of any background gases (empty circles). The baseline fitted to 'uninvolved channels' (solid curve) was subtracted for the composition analysis. See the supplementary information document for more details on how mass spectrometric data was analysed.

the lack of such elevated molecular hydrogen concentrations emitted from the other samples means that the generic presence of elevated molecular hydrogen concentrations in Arctic ice samples cannot be confirmed. As such, this detection in ice sample ICE 2.2 must be considered tentative at best. Furthermore, small quantities of methane and ethane were detected in the ice sample ICE 2.2; however, the amount of methane was found to be less than the uncertainty measured in control experiments and thus is not significant. Similarly, the ethane detected in this ice sample is most likely sourced from outgassing of the plastic vessel used in the experiment (see supplementary information document for more details), and so its presence is also insignificant.

The carbon dioxide content of the deep seawater sample CDT 04 was measured at approximately 6.8%. However, a similar concentration (approximately 6.9%) was measured for the control sample of ultra-pure water that was frozen and then allowed to thaw (Table 4). Yet higher concentrations of carbon dioxide were detected in ice samples ICE 3.1B and ICE 3.9B, which is consistent with their relatively low pH values (Table 2). These ice samples were acquired from the ice-seawater interface and at the air-ice interface, respectively; this observation is consistent with either: (i) these ice samples containing atmospheric carbon dioxide dissolved in the ocean water from which they were formed; or (ii) the oxidation of methane released at the seafloor to carbon dioxide during its ascent, which is then trapped in the surface ice.

To discriminate between these two possible sources, the isotopic composition of carbon dioxide expressed as $\delta^{13}C$ values relative to the Vienna Pee Dee Belemnite (V-PDB) was studied using the signal intensities at the 44 and 45 amu mass channels in the acquired mass spectra. The former is attributed to $^{12}C^{16}O_2$, while the latter is attributed to $^{13}C^{16}O_2$ (with a negligible contribution from $^{12}C^{16}O^{17}O$). For sample ICE 3.1B, the $^{13}CO_2/^{12}CO_2$ ratio was found to be 0.013206 ± 0.001, which equates to a $\delta^{13}C$ value of 1.2 ± 1.4‰. All Arctic samples exhibited $\delta^{13}C$ values that fell into the range of −2.4-2.3‰ (Table 4). The source of these isotopic signatures is not well understood, but it is possible that contributions from various biological processes including methanogenesis (Valentine et al. 2004; Penning et al. 2005; Okumura et al. 2016; Shima et al. 2020) and photosynthesis (Farquhar et al. 1989; Descolas-Gros and Fontungne, 1990; Henderson et al. 2024), as well as various abiotic processes (Kroopnick, 1985; Tagliabue and Bopp, 2008, de la Vega et al., 2019), are at play. The quantification of isotope fractionation effects in other elements (e.g., ^{18}O in H_2O) has also been attempted (Table 4), and our QMS results are in reasonably good agreement with the more accurate data produced through OA-ICOS, albeit with significantly larger uncertainties.

Notably, methane and molecular hydrogen were not detectable in ice samples ICE 3.1B and ICE 3.9B; indeed, the small negative values present in Table 4 may result from background subtraction and indicate that the real uncertainties associated with these measurements may be slightly more significant than those estimated by our analysis. However, the non-detection of reduced molecules in these ice samples is complemented by their apparent enrichment (compared to atmospheric quantities) in molecular oxygen. Lastly, high methane concentrations of about 40% were measured in the gas sample GS 1B, as expected. A small amount (ca. 0.3%) of ethane was also detected in this sample. Although ethane emission from the plastic container used in this experiment is anticipated to be non-negligible (see supplementary information document), the amount of ethane measured in this gas sample is expected to be unaffected by this, since the relatively higher quantities of gas present in this sample compared to gases extracted from the melted ice and seawater samples should dominate over any impurities emitted by the plastic container.

4. Discussion

Methane detected on Enceladus could be produced via the hydrothermal alteration of olivine-rich rocks (i.e., serpentinization; McKay et al. 2012), the thermal alteration of refractory organics (Parnell et al.

Table 4
Abundances and isotopic compositions of trapped or dissolved gases in Arctic ice and seawater samples as measured through QMS analysis.

Sample: ICE 2.2											
Gas	CH_4	C_2H_6	H_2	N_2	O_2	CO_2	Ar	Ne	$\delta^{13}CO_2$ (‰)	$\delta H_2^{18}O$ (‰)	$\delta H_2^{17}O$ (‰)
% Content	0.0678	0.0664	3.5995	72.8516	21.6946	0.7395	1.0642	−0.0837	2.3	1.7	−1.1
Syst. Error	(0.0071)	(0.0032)	(0.0363)	(0.0991)	(0.0108)	(0.0021)	(0.0021)	(0.1109)	(2.1)	(1.2)	(0.6)
Stat. Error	(0.0267)	(0.0478)	(0.0096)	(0.6756)	(0.6756)	(0.6756)	(0.6756)	(0.6756)	(21.1)	(7.5)	(1.9)
Sample: ICE 3.1B											
Gas	CH_4	C_2H_6	H_2	N_2	O_2	CO_2	Ar	Ne	$\delta^{13}CO_2$ (‰)	$\delta H_2^{18}O$ (‰)	$\delta H_2^{17}O$ (‰)
% Content	0.0501	0.4527	0.0291	39.5741	26.1840	32.5119	1.0721	0.1260	1.2	1.9	0.5
Syst. Error	(0.1065)	(0.0496)	(0.0187)	(0.0544)	(0.0130)	(0.0335)	(0.0022)	(0.4222)	(0.02)	(0.2)	(0.1)
Stat. Error	(0.0894)	(0.242)	(0.0336)	(0.0924)	(0.1095)	(0.1483)	(0.0890)	(3.3375)	(1.4)	(2.8)	(0.3)
Sample: ICE 3.9B											
Gas	CH_4	C_2H_6	H_2	N_2	O_2	CO_2	Ar	Ne	$\delta^{13}CO_2$ (‰)	$\delta H_2^{18}O$ (‰)	$\delta H_2^{17}O$ (‰)
% Content	−0.3093	0.1138	−0.3498	48.3328	26.7371	25.3824	1.0859	−0.9929	−1.6	0.7	0.21
Syst. Error	(0.0309)	(0.019)	(0.0073)	(0.0663)	(0.0133)	(0.0264)	(0.0022)	(0.2439)	(0.2)	(0.2)	(0.05)
Stat. Error	(0.0511)	(0.1249)	(0.0198)	(0.0649)	(0.0670)	(0.0818)	(1.7327)	(1.7327)	(1.6)	(1.2)	(0.30)
Sample: GS 1B											
Gas	CH_4	C_2H_6	H_2	N_2	O_2	CO_2	Ar	Ne	$\delta^{13}CO_2$ (‰)	$\delta H_2^{18}O$ (‰)	$\delta H_2^{17}O$ (‰)
% Content	40.0964	0.3342	−0.4047	44.8096	13.4310	2.2123	0.6751	−1.1538	2.1	1.7	1.6
Syst. Error	(0.1239)	(0.0347)	(0.0026)	(0.0616)	(0.0067)	(0.0031)	(0.0014)	(0.1262)	(1.0)	(0.6)	(0.1)
Stat. Error	(0.2211)	(0.3594)	(0.0516)	(0.1494)	(0.1559)	(0.2157)	(0.1435)	(4.9224)	(70.1)	(6.7)	(1.7)
Sample: CTD 04											
Gas	CH_4	C_2H_6	H_2	N_2	O_2	CO_2	Ar	Ne	$\delta^{13}CO_2$ (‰)	$\delta H_2^{18}O$ (‰)	$\delta H_2^{17}O$ (‰)
% Content	−0.2945	−0.1431	−0.3834	69.7990	25.6588	4.9880	1.2689	−0.8937	−2.4	0.4	0.4
Syst. Error	(0.1432)	(0.0239)	(0.0123)	(0.0957)	(0.0127)	(0.0084)	(0.0025)	(0.3603)	(4.4)	(0.2)	(0.1)
Stat. Error	(0.1342)	(0.1999)	(0.0293)	(0.1032)	(0.0999)	(0.1133)	(0.0719)	(2.7343)	(23.0)	(1.3)	(0.3)
Sample: Ultra-pure water that was frozen and allowed to rethaw (control)											
Gas	CH_4	C_2H_6	H_2	N_2	O_2	CO_2	Ar	Ne	$\delta^{13}CO_2$ (‰)	$\delta H_2^{18}O$ (‰)	$\delta H_2^{17}O$ (‰)
% Content	−0.7189	22.9873	−0.1080	43.7050	24.7512	7.1731	1.2837	0.9266	10.2	0.6	0.4
Syst. Error	(0.3109)	(0.3491)	(0.0450)	(0.0601)	(0.0124)	(0.0247)	(0.0026)	(1.0115)	(3.1)	(0.2)	(0.1)
Stat. Error	(0.5157)	(0.6966)	(0.1180)	(0.2586)	(0.2833)	(0.2684)	(0.2088)	(9.8937)	(25.8)	(1.6)	(0.4)

2005; Oehler and Etiope, 2017), or possibly by microbial metabolism; particularly methanogenesis led by hydrogenotrophic methanogenic archaea-like organisms (McKay et al. 2012; Mitri et al. 2018; Taubner et al. 2018; Kotlarz et al. 2020; Affholder et al. 2022). Once produced by any of the above-listed biological or abiotic pathways, methane could then conceivably undergo anaerobic oxidation by methanotrophic or sulphate-reducing microbial metabolisms (Boetius et al. 2000; Teichert et al. 2005). The by-products of this hypothesised microbial activity on Enceladus would be authigenic carbonates and sulphides that precipitate within shallow sediments or at the sediment-water interface. Such methane-derived carbonate deposits may show microbially-mediated mineral phases and cements having strongly negative $\delta^{13}C$ values arising from the anaerobic oxidation of methane (Boetius et al. 2000; Aloisi et al. 2002; Knittel and Boetius, 2009). Therefore, if chemosynthetic life based on methane cycling ever existed on Enceladus, the most direct evidence for it should be found in its vent and seep systems and the carbonates associated with the dissociation of gas hydrates (Carrizo et al. 2022). This poses a serious technical problem for assessing the past and present habitability of Enceladus, since such evidence would exist at the seafloor below a typical ice covering of ca. 35–40 km in thickness. Therefore, another strategy for future astrobiology missions to Enceladus might be to directly sample the emergent plume or the surface ice shell.

Molecular hydrogen may also be regarded as indirect geochemical evidence of biologically mediated methane cycling occurring beneath Enceladus' icy shell, and is in fact consistent with the high abundance of molecular hydrogen already measured in its southern pole plume (Waite et al. 2017; Ray et al. 2021): molecular hydrogen could be produced by the hydrolysis of olivine and become the substrate for chemolithoautotrophic consortia living in vent and seep environments (Waite et al. 2017; Taubner et al. 2018; Ray et al. 2021; Affholder et al. 2022). Our experiments have tentatively demonstrated that the concentration of molecular hydrogen in one ice sample (ICE 2.2) acquired from the Arctic Ocean (a suitable terrestrial analogue for Enceladus) is ca. 3.6%, which is about 175 times higher than its concentration in laboratory air control samples that were analysed (0.02%), and is ca. 2.5–10 times higher than molecular hydrogen concentrations observed in the southern pole plume of Enceladus (0.4–1.4% volume mixing ratio; Waite et al. 2017). This high concentration of molecular hydrogen in this Arctic Ocean ice sample could possibly be sourced from hydrothermal activity linked to serpentinization along the Arctic mid-oceanic ridge (Waite et al. 2017; Kotlarz et al. 2020). Although only one of our Arctic Ocean ice samples exhibited this enrichment in molecular hydrogen, this preliminary result nevertheless suggests that hydrothermal activity within the global ocean of Enceladus might be inferred from excesses of molecular hydrogen within its ice shell.

Offshore western Svalbard is a unique environment for performing experiments and collecting samples that are relevant to Enceladus: in this environment, there are several sources of microbial and thermogenic methane, including gas hydrate settings such as the Vestnesa Ridge considered here (Panieri et al. 2017, Pape et al., 2020) as well as hydrothermally active regions such as the Jøtul vent field from which previous headspace gas analyses has provided evidence for thermogenic methane generated at higher temperatures (Bohrmann et al. 2024). However, as shown by the present study, the identification of even indirect evidence of methane seepage and biological activity in Arctic Ocean ice analogues may be very challenging using QMS methods similar to those likely to be included in the payloads of future missions. Indeed, we were not able to detect any methane in our Arctic Ocean ice analogues despite their unequivocal association with hydrocarbons (i.e., natural gas), and thus were unable to measure any isotopic fractionations in reduced carbon that would indicate a biological or abiotic origin. The reason for this non-detection of methane is not well understood, but it might be related to the Earth's oceans having a strong oxidative potential that rapidly induces the dissociation of methane (Reeburgh, 2007; Morris et al. 2022). This might be one of the intrinsic limitations of running these experiments using ice analogues from Earth; however, the *Cassini-Huygens* mission indicated through its detection of methane in cryovolcanic plumes (Waite et al. 2006) that such a scenario does not exist on Enceladus, and so it is possible, at least in principle, that mass spectrometric equipment aboard future missions could measure methane abundances and isotopic compositions directly on the Enceladus ice shell. To support these ambitions, we have been able to use QMS methods to determine the carbon isotopic composition of

methane in the gas sample GS 1B to be $\delta^{13}C = [1.8 \pm 2.0$ (syst.) ± 4.1 (stat.)].

Moreover, we have been able to successfully measure the carbon isotopic content of carbon dioxide and the oxygen isotopic content of water vapour emitted by the melted ice and seawater samples through QMS measurements since, in the case of carbon dioxide, the mass channels for the relevant isotopologues are relatively free from overlap with those of other molecules of immediate interest to Enceladus; while in the case of water, an advanced methodology may be applied (see supplementary information document for more information). These measurements were admittedly characterised by relatively high statistical uncertainties (Table 4) which may preclude the identification of specific processes contributing to the fractionation of a particular isotope system; however, the comparatively smaller systematic uncertainties nonetheless go some way towards demonstrating that the isotopic compositional analysis of the molecular constituents of Enceladus' icy shell by mass spectrometric instrumentation likely to be aboard future missions may indeed be possible with sufficiently long measurements and further method refinement.

Our findings are particularly relevant when considering the growing number of potential future fly-by missions to Enceladus, such as the *Enceladus Life Finder* (Reh et al. 2016), *Moonraker* (Mousis et al. 2022), and instruments specifically designed for working on ice samples, such as the Exobiology Extant Life Surveyor (EELS, Vaquero et al., 2024). Both *Enceladus Life Finder* and *Moonraker* plan to include payloads containing mass spectrometers (EELS is unlikely to have a mass spectrometer in its payload) that will be able to investigate the composition of cryovolcanic plume material in the hopes of detecting organic molecules or biosignatures within ice crystals (Reh et al. 2016; Mitri et al. 2018, 2021). For instance, the *Enceladus Life Finder* mission is planned to include mass spectrometers for the analysis of both gases (the Mass Spectrometer for Planetary Exploration – MASPEX) as well as ice and dust grains (the Enceladus Icy Jet Analyser – ENIJA) from the southern pole plume (Reh et al. 2016). Similarly, the proposed *Moonraker* mission plans to include an Ion and Neutral Mass Spectrometer (M-INMS) for measuring the gas-phase and thermal ion population around Enceladus as well as a High Ice Flux Instrument (HIFI) for measuring plume ice grain compositions via impact-ionisation time-of-flight mass spectrometry (Mousis et al. 2022). Of course, our results may also have implications for the analysis of data collected during fly-bys of other outer Solar System ocean worlds, such as the Jovian moons Europa and Ganymede which will be studied in detail by the *Europa Clipper* and *Jupiter Icy Moons Explorer* (JUICE) missions (Grasset et al. 2013; Pappalardo et al. 2024).

5. Conclusions

For the first time, ice from the Arctic pack has been considered as a terrestrial analogue of part of an outer Solar System icy moon for astrobiological research. We have conducted experiments on the composition of trapped gases that are emitted from Arctic ice and seawater samples analogous to those that may be found on Enceladus using mass spectrometric techniques that are comparable with the planned payloads of future robotic missions to this ice-capped ocean world. These experiments were motivated by the desire to search for biosignatures associated with possible microbially mediated methane cycling in sub-surface seep and vent environments in the ice shell and plume materials. Our results found no unequivocal traces of methane in the Arctic analogues (despite their known association with hydrocarbon-rich terrestrial environments), possibly due to inherent limitations of our terrestrial analogue and laboratory analysis. However, we were able to successfully measure emitted carbon dioxide concentrations and associated carbon isotopic abundances, as well as oxygen isotopic compositions in water, indicating that such measurements may be possible by mass spectrometric equipment aboard the payloads of future missions to Enceladus. We also tentatively identified an excess of molecular hydrogen in an Arctic ice sample with abundances comparable to previous compositional analyses of Enceladus' southern pole plume, which could be used as possible indirect evidence of putative hydrogenotrophic methanogenic ecosystems at the seafloor. Our results therefore justify future studies and attempts at method development and refinement.

CRediT authorship contribution statement

F. Franchi: Writing – review & editing, Writing – original draft, Project administration, Investigation, Funding acquisition, Formal analysis, Conceptualization. **M. Túri:** Methodology, Formal analysis. **G. Lakatos:** Formal analysis, Data curation. **K.K. Rahul:** Formal analysis, Data curation. **D.V. Mifsud:** Writing – review & editing, Writing – original draft, Methodology, Investigation, Data curation. **G. Panieri:** Writing – review & editing, Resources, Project administration, Funding acquisition. **R. Rácz:** Methodology, Formal analysis. **S.T.S. Kovács:** Methodology, Formal analysis, Data curation. **E. Furu:** Formal analysis, Data curation. **R. Huszánk:** Formal analysis, Data curation. **R.W. McCullough:** Software, Methodology. **Z. Juhász:** Writing – review & editing, Writing – original draft, Validation, Software, Methodology, Investigation, Formal analysis, Data curation, Conceptualization.

Declaration of competing interest

The authors declare that they have no known competing financial interests or personal relationships that could have appeared to influence the work reported in this paper.

Acknowledgements

The authors gratefully acknowledge the Europlanet 2024 RI which has been funded by the European Union Horizon 2020 Research Innovation Programme under grant agreement no. 871149. This work is also based on work from the COST Action CA20129 MultIChem, supported by COST (European Cooperation in Science and Technology). The Norwegian Research Council supported the AKMA2-OceanSenses expedition and data collection through the AKMA Project (Advancing Knowledge of Methane in the Arctic; project no. 287869). Zoltán Juhász acknowledges support from the Hungarian Academy of Sciences through the János Bolyai Research Scholarship. We are grateful to Eva E. Stüeken (University of St Andrews, United Kingdom) for her useful comments and feedback that improved the quality of this manuscript. We are also grateful to Dimitri Kalenitchenko (La Rochelle Université, France) for his guidance on ice sampling and preparation.

Appendix A. Supplementary data

Supplementary data to this article can be found online at https://doi.org/10.1016/j.pss.2025.106051.

Data availability

Data will be made available on request.

References

Affholder, A., Guyot, F., Sauterey, B., Ferrière, R., Mazevet, S., 2022. The Planetary Science Journal 3, 270.
Aloisi, G., Bouloubassi, I., Heijs, S.K., Pancost, R.D., Pierre, C., Sinninghe Damsté, J.S., Gottschal, J.C., Forney, L.J., Rouchy, J.M., 2002. Earth Planet Sci. Lett. 203, 195.
Boetius, A., Ravenschlag, K., Schubert, C.J., Rickert, D., Widdel, F., Gieseke, A., Amann, R., Jørgensen, B.B., Witte, U., Pfannkuche, O., 2000. Nature 407, 623.
Bohrmann, G., Streuff, K., Römer, M., Knutsen, S.M., Smrzka, D., Kleint, J., Röhler, A., Pape, T., Sandstå, N.R., Kleint, C., Hansen, C., Ferreira, C dos Santos, Walter, M., Macedo de Paula Santos, G., Bach, W., 2024. Sci. Rep. 14, 10168.
Bouquet, A., Mousis, O., Waite, J.H., Picaud, S., 2015. Geophys. Res. Lett. 42, 1334.

Bünz, S., Polyanov, S., Vadakkepuliyambatta, S., Consolaro, C., Mienert, J., 2012. Mar. Geol. 332–334, 187–197.
Cable, M.L., Porco, C., Glein, C.R., German, C.R., MacKenzie, S.M., Neveu, M., Hoehler, T.M., Hofmann, A.E., Hendrix, A.R., Eigenbrode, J., Postberg, F., Spilker, L. J., McEwen, A., Khawaja, N., Waite, J.H., Wurz, P., Helbert, J., Anbar, A., Vera, JP de, Núñez, J., 2021. The Planetary Science Journal 2, 132.
Carrizo, D., de Dios-Cubillas, A., Sánchez-García, L., López, I., Prieto-Ballasteros, O., 2022. Astrobiology 22, 552.
Coplen, T.B., 1994. Pure Appl. Chem. 66, 273.
Coplen, T.B., 2004. Laboratory information management system (LIMS). Announcement of a Practical Training Session on its Use.
Dannenmann, M., Klenner, F., Bönigk, J., Pavlista, M., Napoleoni, M., Hillier, J., Khawaja, N., Olsson-Francis, K., Cable, M.L., Malaska, M.J., Abel, B., Postberg, F., 2023. Astrobiology 23, 60–75.
de la Vega, C., Jeffreys, R.M., Tuerena, R., Ganeshram, R., 2019. Global Change Biol. 25, 4116.
Descolas-Gros, C., Fontungne, M., 1990. Plant Cell Environ. 13, 207.
Douglas, P.M.J., Stolper, D.A., Eiler, J.M., Sessions, A.L., Lawson, M., Shuai, Y., Bishop, A., Podlaha, O.G., Ferreira, A.A., Santos Neto, E.V., Niemann, M., Steen, A.S., Huang, L., Chimiak, L., Valentine, D.L., Fiebig, J., Luhmann, A.J., Seyfried, W.E., Etiope, G., Schoell, M., Inskeep, W.P., Moran, J.J., Kitchen, N., 2017. Org. Geochem. 113, 262–282.
Eiken, O., Hinz, K., 1993. Sediment. Geol. 82, 15.
Engen, O., Faleide, J.I., Dyreng, T.K., 2008. Tectonophysics 450, 51.
Farquhar, G.D., Ehleringer, J.R., Hubick, K.T., 1989. Annu. Rev. Plant Physiol. Plant Mol. Biol. 40, 503.
Grasset, O., Dougherty, M.K., Coustenis, A., Bunce, E.J., Erd, C., Titov, D., Blanc, M., Coates, A., Drossart, P., Fletcher, L.N., Hussmann, H., Jaumann, R., Krupp, N., Lebreton, J.P., Prieto-Ballesteros, O., Tortora, P., Tosi, F., Hoolst, T Van, 2013. Planet. Space Sci. 78, 1–21.
Hemingway, D., Iess, L., Taieddine, R., Tobie, G., 2018. The interior of Enceladus. In: Schenk, P.M., Clark, R.N., Howett, C.J.A., Verbiscer, A.J., Waite, J.H. (Eds.), Enceladus and the Icy Moons of Saturn. University of Arizona Press, Tucson AZ (United States), pp. 57–77.
Henderson, L.C., Wittmers, F., Carlson, C.A., Worden, A.Z., Close, H.G., 2024. Proceedings of the National Academy of Sciences of the USA 121, e2304613121.
Herr, F.L., 1984. Tellus B 36B (1).
Herr, F.L., Scranton, M.I., Barger, W.R., 1981. Deep-Sea Res. A 28, 1001.
Himmler, T., Sahy, D., Martma, T., Bohrmann, G., Plaza-Faverola, A., Bünz, S., Condon, D.J., Knies, J., Lepland, A., 2019. Sci. Adv. 5, aaw1450.
Hsu, H.W., Postberg, F., Sekine, Y., Shibuya, T., Kempf, S., Horányi, M., Juhász, A., Altobelli, N., Suzuki, K., Masaki, Y., Kuwatani, T., Tachibana, S., Sirono, S., Moragas-Klostermeyer, G., Srama, R., 2015. Nature 519, 207.
Iess, L., Stevenson, D.J., Parisi, M., Hemingway, D., Jacobsen, R.A., Lunine, J., Nimmo, F., Armstrong, J., Asmar, S., Ducci, M., Tortora, P., 2014. Science 344, 78.
James, R.H., Bousquet, P., Bussmann, I., Haeckel, M., Kipfer, R., Leifer, I., Niemann, H., Ostrovsky, I., Piskozub, J., Rehder, G., Treude, T., Vielstädte, L., Greinert, J., 2016. Limnol. Oceanogr. 61, S283.
Khawaja, N., Postberg, F., Hillier, J., Klenner, F., Kempf, S., Nölle, L., Reviol, R., Zou, Z., Srama, R., 2019. Mon. Not. Roy. Astron. Soc. 489, 5231–5243.
Klenner, F., Bönigk, J., Napoleoni, M., Hillier, J., Khawaja, N., Olsson-Francis, K., Cable, M.L., Malaska, M.J., Kempf, S., Abel, B., Postberg, F., 2024. Sci. Adv. 10, eadl0849.
Knittel, K., Boetius, A., 2009. Annu. Rev. Microbiol. 63, 311.
Kotlarz, J., Zielenkiewicz, U., Zalewska, N.E., Kubiak, K.A., 2020. Astrophysical Bulletin 75, 166.
Kroopnick, P.M., 1985. Deep-Sea Res. A 32, 57.
Lehmann, M., Siegenthaler, U., 1991. J. Glaciol. 37, 23–26.
MacKenzie, S.M., Neveu, M., Davila, A.F., Lunine, J.I., Craft, K.L., Cable, M.L., Phillips-Lander, C.M., Hofgartner, J.D., Eigenbrode, J.L., Waite, J.H., Glein, C.R., 2021. The Planetary Science Journal 2, 77.
Marion, G.M., Millero, F.J., Camões, M.F., Spitzer, P., Feistel, R., Chen, C.T.A., 2011. Mar. Chem. 126, 89.
Mayhew, L.E., Ellison, E.T., McCollom, T.M., Trainor, T.P., Templeton, A.S., 2013. Nat. Geosci. 6, 478–484.
McCollom, T.M., Seewald, J.S., 2006. Earth Planet Sci. Lett. 243, 74.
McKay, C.P., Khare, B.N., Amin, R., Klasson, M., Kral, T.A., 2012. Planet. Space Sci. 71, 73.
Milkov, A.V., Etiope, G., 2018. Org. Geochem. 125, 109.
Mitri, G., Postberg, F., Soderblom, J.M., Wurz, P., Tortora, P., Abel, B., Barnes, J.W., Berga, M., Carrasco, N., Coustenis, A., de Vera, J.P.P., D'Ottavio, A., Ferri, F., Hayes, A.G., Hayne, P.O., Hillier, J.K., Kempf, S., Lebreton, J.P., Lorenz, R.D., Martelli, A., Orosei, R., Petropoulos, A.E., Reh, K., Schmidt, J., Sotin, C., Srama, R., Tobie, G., Vorburger, A., Vuitton, V., Wong, A., Zannoni, M., 2018. Planet. Space Sci. 155, 73.
Mitri, G., Barnes, J., Coustenis, A., Flamini, E., Hayes, A., Lorenz, R.D., Mastrogiuseppe, M., Orosei, R., Postberg, F., Reh, K., Soderblom, J.M., Sotin, C., Tobie, G., Tortora, P., Vuitton, V., Wurz, P., 2021. Experimental Astronomy, pp. 1–34.
Morris, J.J., Rose, A.L., Lu, Z., 2022. Redox Biol. 52, 102285.
Mousis, O., Bouquet, A., Langevin, Y., et al., 2022. The Planetary Science Journal 3, 268.
Oehler, D.Z., Etiope, G., 2017. Astrobiology 17, 1233.
Okumura, T., Kawaguchi, S., Saito, Y., Matsui, Y., Takai, K., Imachi, H., 2016. Prog. Earth Planet. Sci. 3, 14.
Orr, J.C., Fabry, V.J., Aumont, O., Bopp, L., Doney, S.C., Feely, R.A., Gnanadesikan, A., Gruber, N., Ishida, A., Joos, F., Key, R.M., Lindsay, K., Maier-Reimer, E., Matear, R., Monfray, P., Mouchet, A., Najjar, R.G., Plattner, G.K., Rodgers, K.B., Sabine, C.L., Sarmiento, J.L., Schiltzer, R., Slater, R.D., Totterdell, I.J., Weirig, M.F., Yamanaka, Y., Yool, A., 2005. Nature 437, 681–686.
Oze, C., Sharma, M., 2005. Geophys. Res. Lett. 32, L10203.
Panieri, G., Bünz, S., Fornari, D.J., Escartin, J., Serov, P., Jansson, P., Torres, M.E., Johnson, J.E., Hong, W.L., Sauer, S., Garcia, R., Gracias, N., 2017. Mar. Geol. 390, 282–300.
Panieri, G., Bünz, S., Savini, A., Jensen, A., Løfquist, B., Olsen, B.R., Willis, C., Argentino, C., Bertin, C., Oddone, D., Kalenitchenko, D., Rosnes, E., Cusset, F., Maric, F., Franchi, F., Pawlowski, J., Zimmermann, J., Todd, J.E., Meyer, J.P., Waghorn, K.A., Losleben, L.K., Poto, M.P., Eilertsen, M.H., Stiller-Reeve, M.A., Clerici, M., Dessandier, P.A., Moncelon, R., Ramalho, S., Mohadjer, S., Vågenes, S., Aune, V., Os, V., Poddevin, V., Holm, V.D., 2022. CAGE22-2 scientific cruise report: AKMA 2/Ocean Senses. CAGE – Centre for Arctic Gas Hydrate, Environment, and Climate Report Series 10.
Pape, T., Bünz, S., Hong, W.L., Torres, M.E., Riedel, M., Panieri, G., Lepland, A., Hsu, C. W., Wintersteller, P., Wallmann, K., Schmidt, C., Yao, H., Bohrmann, G., 2020. J. Geophys. Res. Solid Earth 125, e2018JB016679.
Pappalardo, R.T., Buratti, B.J., Korth, H., et al., 2024. Space Sci. Rev. 220, 40.
Park, R.S., Mastrodemos, N., Jacobsen, R.A., Berne, A., Vaughan, A.T., Hemingway, D.J., Leonard, E.J., Castillo-Rogez, J.C., Cockell, C.S., Keane, J.T., Konopliv, A.S., Nimmo, F., Riedel, J.E., Simons, M., Vance, S., 2024. J. Geophys. Res.: Planets 129, e2023JE008054.
Parnell, J., Osinski, G.R., Green, P Le, Baron, M.J., 2005. Geology 33, 373.
Penning, H., Plugge, C.M., Galand, P.E., Conrad, R., 2005. Global Change Biol. 11, 2103.
Plaza-Faverola, A., Bünz, S., Johnson, J.E., Chand, S., Knies, J., Mienert, J., Franek, P., 2015. Geophys. Res. Lett. 42, 733.
Porco, C.C., Helfenstein, P., Thomas, P.C., Ingersoll, A.P., Wisdom, J., West, R., Neukum, G., Denk, T., Wagner, R., Roatsch, T., Kieffer, S., Turtle, E., McEwen, A., Johnson, T.V., Rathbun, J., Veverka, J., Wilson, D., Perry, J., Spitale, J., Brahic, A., Burns, J.A., DelGenio, A.D., Dones, L., Murray, C.D., Squyres, S., 2006. Science 311, 1393.
Posewang, J., Mienert, J., 1999. Geo Mar. Lett. 19, 150.
Postberg, F., Kempf, S., Schmidt, J., Brilliantov, N., Beinsen, A., Abel, B., Buck, U., Srama, R., 2009. Nature 459, 1098.
Postberg, F., Schmidt, J., Hillier, J., Kempf, S., Srama, R., 2011. Nature 474, 620.
Postberg, F., Khawaja, N., Abel, B., Choblet, G., Glein, C.R., Gudipati, M.S., Henderson, B. L., Hsu, H.W., Kempf, S., Klenner, F., Moragas-Klostermeyer, G., Magee, B., Nölle, L., Perry, M., Reviol, R., Schmidt, J., Srama, R., Stolz, F., Tobie, G., Trieloff, M., Waite, J.H., 2018. Nature 558, 564–568.
Postberg, F., Sekine, Y., Klenner, F., Glein, C.R., Zou, Z., Abel, B., Furuya, K., Hillier, J.K., Khawaja, N., Kempf, S., Noelle, L., Saito, T., Schmidt, J., Shibuya, T., Srama, R., Tan, S., 2023. Nature 6181, 489–493.
Rácz, R., Kovács, S.T.S., Lakatos, G., Rahul, K.K., Mifsud, D.V., Herczku, P., Sulik, B., Juhász, Z., Perduk, Z., Ioppolo, S., Mason, N.J., Field, T.A., Biri, S., McCullough, R. W., 2024. Rev. Sci. Instrum. 95, 095105.
Ray, C., Glein, C.R., Waite, J.H., Teolis, B., Hoehler, T., Huber, J.A., Lunine, J., Postberg, F., 2021. Icarus 364, 114248.
Raza, A., Deen, K.M., Asselin, E., Haider, W., 2022. Renew. Sustain. Energy Rev. 161, 112323.
Reeburgh, W.S., 2007. Chem. Rev. 107, 486.
Reh, K., Spilker, L., Lunine, J.I., Waite, J.H., Cable, M.L., Postberg, F., Clark, K., 2016. Enceladus Life Finder: the Search for Life in a Habitable Moon. 2016 IEEE Aerospace Conference, IEEE, pp. 1–8.
Riding, R., Virgone, A., 2020. Earth Sci. Rev. 208, 103300.
Shima, S., Huang, G., Wagner, T., Ermler, U., 2020. Annu. Rev. Microbiol. 74, 713.
Souchez, R., Tison, J.L., 1987. Geophys. Res. Lett. 14, 599–602.
Srama, R., Ahrens, T.J., Altobelli, N., Auer, S., Bradley, J.G., Burton, M., Dikarev, V.V., Economou, T., Fechtig, H., Görlig, M., Grande, M., Graps, A., Grün, E., Havnes, O., Helfert, S., Horanyi, M., Igenbergs, E., Jessberger, E.K., Johnson, T.V., Kempf, S., Krivov, A.V., Krüger, H., Mocker-Ahlreep, A., Moragas-Klostermeyer, G., Lamy, P., Landgraf, M., Linkert, D., Linkert, G., Lura, F., McDonnell, J.A.M., Möhlmann, D., Morfill, G.E., Müller, M., Roy, M., Schäfer, G., Schlotzhauer, G., Schwehm, G.H., Spahn, F., Stübig, M., Svestka, J., Tschernjawski, V., Tuzzolino, A.J., Wäsch, R., Zook, H.A., 2004. Space Sci. Rev. 114, 465–518.
Tagliabue, A., Bopp, L., 2008. Global Biogeochem. Cycles 22, GB1025.
Taubner, R.S., Pappenreiter, P., Zwicker, J., Smrzka, D., Pruckner, C., Kolar, P., Bernacchi, S., Seifert, A.H., Krajete, A., Bach, W., Peckmann, J., Paulik, C., Firneis, M.G., Schleper, C., Rittmann, S.K.M.R., 2018. Nat. Commun. 9, 748.
Teichert, B.M.A., Bohrmann, G., Seuss, E., 2005. Palaeogeogr. Palaeoclimatol. Palaeoecol. 227, 67.
Toyota, T., Smith, I.J., Gough, A.J., Langhorne, P.J., Leonard, G.H., van Hale, R.J., Mahoney, A.R., Haskell, T.G., 2013. J. Glaciol. 59, 697–710.
Valentine, D.L., Chidthaisong, A., Rice, A., Reeburgh, W.S., Tyler, S.C., 2004. Geochem. Cosmochim. Acta 68, 1571.
Vanneste, M., Guidard, S., Mienert, J., 2005. Terra. Nova 17, 510.
Vaquero, T.S., Daddi, G., Thakker, R., Paton, M., Jasour, A., Strub, M.P., Swan, R.M., Royce, R., Gildner, M., Tosi, P., Veismann, M., Gavrilov, P., Marteau, E., Bowkett, J., Lemus, D Loret de Mola, Nakka, Y., Hockman, B., Orekhov, A., Hasseler, T.D., Leake, C., Nuernberger, B., Proença, P., Reid, W., Talbot, W., Georgiev, N., Pailevanian, T., Archanian, A., Ambrose, E., Jasper, J., Etheredge, R., Roman, C., Levine, D., Otsu, K., Yearicks, S., Melikyan, H., Rieber, R.R., Carpenter, K., Nash, J., Jain, A., Shiraishi, L., Robinson, M., Travers, M., Choset, H., Burdick, J., Gardner, A., Cable, M., Ingham, M., Ono, M., 2024. Science Robots 9, eadh8332.
Veselý, L., Štůsek, R., Mikula, O., Yang, X., 2024. Sci. Total Environ. 946, 174194.

Waite, J.H., Lewis, W.S., Kasprzak, W.T., Anicich, V.G., Block, B.P., Cravens, T.E., Fletcher, G.G., Ip, W.H., Luhmann, G.H., McNutt, R.L., Niemann, H.B., 2004. The Cassini ion and neutral mass spectrometer (INMS) investigation. In: Russell, C.T. (Ed.), The Cassini-Huygens Mission. Springer Nature, Berlin (Germany), pp. 113–231.

Waite, J.H., Combi, M.R., Ip, W.H., Cravens, T.E., McNutt, R.L., Kasprzak, W., Yelle, R., Luhmann, J., Niemann, H., Gell, D., Magee, B., Fletcher, G., Lunine, J., Tseng, W.L., 2006. Science 311, 1419–1422.

Waite, J.H., Glein, C.R., Perryman, R.S., Teolis, B.D., Magee, B.A., Miller, G., Grimes, J., Perry, M.E., Miller, K.E., Bouquet, A., Lunine, J.I., Brockwell, T., Bolton, S.J., 2017. Science 356, 155.

Wang, D.T., Gruen, D.S., Sherwood Lollar, B., Hinrichs, K.U., Stewart, L.C., Holden, J.F., Hristov, A.N., Pohlman, J.W., Morrill, P.L., Könneke, M., Delwiche, K.B., Reeves, E. P., Sutcliffe, C.N., Ritter, D.J., Seewald, J.S., McIntosh, J.C., Hemond, H.F., Kubo, M. D., Cardace, D., Hoehler, T.M., Ono, S., 2015. Science 348, 428–431.